Analytical Methods

Accepted Manuscript

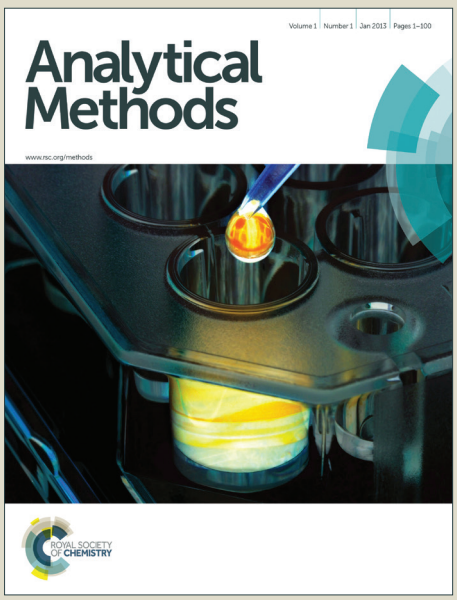

ROYAL SOCIETY OF CHEMISTRY

www.rsc.org/methods

Electrochemically synthesized partially reduced graphene oxide modified glassy carbon electrode for individual and simultaneous voltammetric determination of ascorbic acid, dopamine and uric acid

Padamadathil K. Aneesh, Sindhu R. Nambiar, Talasila P. Rao*, Ayyappanpillai Ajayaghosh

Graphical Abstract

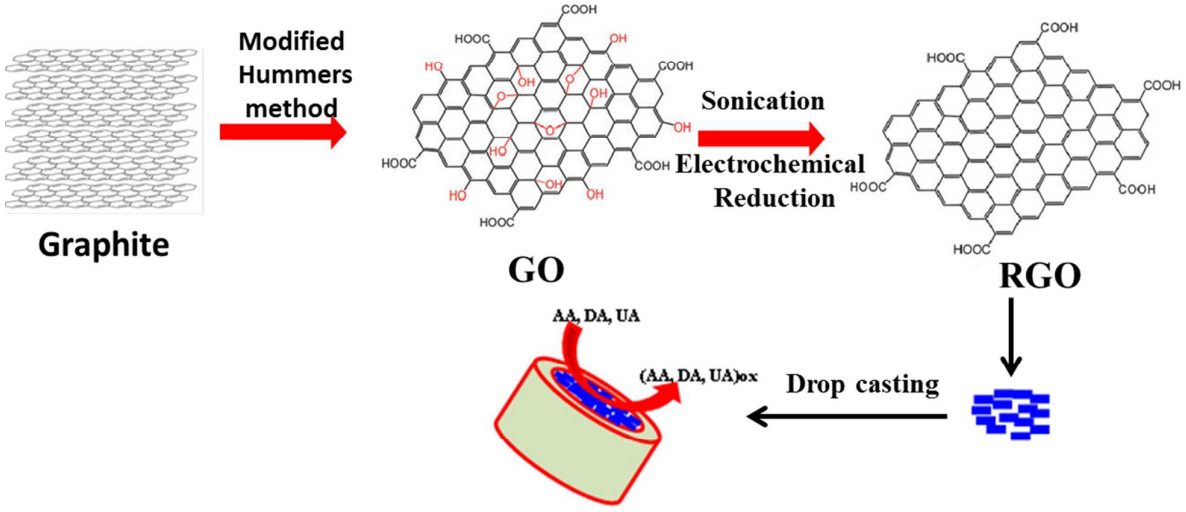

- Electrochemically reduced graphene oxide modified glassy carbon electrode with good sensitivity and selectivity were developed and applied for sensing AA, DA and UA.

Electrochemically synthesized partially reduced graphene oxide modified glassy carbon electrode for individual and simultaneous voltammetric determination of ascorbic acid, dopamine and uric acid

Padamadathil K. Aneesh, Sindhu R. Nambiar, Talasila P. Rao*, Ayyappanpillai Ajayaghosh

Chemical Sciences and Technology Division (CSTD)

CSIR-National Institute for Interdisciplinary Science and Technology (CSIR-NIIST)

Trivandrum 695019, India

Abstract

We report here an efficient and simple approach for the preparation of partially reduced graphene oxide modified glassy carbon electrode (RGO-GCE). The modification of RGO-GCE consists of three steps. This includes (i) chemical synthesis of graphite oxide by modified Hummer's method (ii) exfoliation of graphite oxide to graphene oxide (GO) by ultra-sonication and (iii) controlled partial electrochemical reduction in 0.1M phosphate buffered medium (pH 3.0) via potentiodynamic cycling (2 cycles) to obtain partially reduced graphene oxide modified glassy carbon electrode (RGO-GCE). The behaviour of RGO-GCE towards ascorbic acid (AA), dopamine (DA) and uric acid (UA) was investigated by differential pulse voltammetry, with enrichment time of 3 minutes. This showed that modified electrode has good precision (1.42, 1.92 and 2.20 % for AA, DA and UA, respectively) and resolution at pH 3.0 for all the three molecules which enable their individual and simultaneous determination. Under the optimized conditions, the electrochemical sensor showed a wider linear response for AA, DA and UA in the concentration ranges of 4×10^{-5} to 1×10^{-3} M, 1×10^{-7} to 1×10^{-4} M and 8×10^{-7} to 8×10^{-4} M with detection limits of 4.2×10^{-6}, 8×10^{-9} and 6×10^{-7} M, respectively based on 3 times the standard deviation of the blank with minimum fouling effect. Detailed spectral (IR & Raman), morphological (SEM and TEM) and electrochemical characterization studies were also reported. Finally, the performance of RGO-GCE based sensor was successfully tested for analysing UA and quantitative recoveries of AA and DA in serum samples.

Keywords: Partially reduced graphene oxide, electrochemical reduction, differential pulse voltammetry.

Corresponding Author Email: tprasadarao07@gmail.com

Introduction

Ascorbic acid (AA), Dopamine (DA) and Uric acid (UA) are compounds of great biomedical interest having potential role in human metabolism. Among the animal organs, liver, leukocytes, and anterior pituitary lobe show the highest concentration of AA. It is widely used in food and drinks as an antioxidant and is a vital component in human diet [1]. Dopamine is one of the most important catecholamine neurotransmitters in the central nervous system of mammals and its biochemistry is believed to be related to several diseases, such as schizophrenia and parkinsonism [2]. Uric acid is the primary end product of purine metabolism and its abnormal levels are symptoms of several diseases such as gout, hyperuricemina, and Lesch-Nyan disease [3]. The concentration of DA in extracellular fluid of the caudate nucleus is extremely low (1×10^{-8} - 1×10^{-6} M) for a healthy individual and even lower levels (1×10^{-9} M), in patients suffering with parkinson's disease, whereas the concentration of AA and UA is 2-3 orders of higher magnitude than DA [4]. As AA, DA and UA plays important role in the human body, and often coexists in biological fluids, the rapid, cost-effective, sensitive, selective and simultaneous detection of these three species have always been of great research interest [5]. In recent years, the study of the electrochemical behaviour of bioactive molecules has become one of the most exciting developments in the fields of electrochemistry and electroanalytical chemistry because of its simplicity, short analysis time, low cost, portability and wider calibration range over other sensing methods [6]. Therefore, electrochemical determination methods for AA, DA and UA must be developed in conjunction with a suitable modification material that facilitates complete

resolution of their electrochemical signals, or the selective detection of at least one analyte without the influence from others.

Graphene and related materials such as graphene oxide, reduced graphene oxide etc have grabbed great attention since its successful isolation in 2004 [7]. It is a fascinating single-atom-thick and two-dimensional carbon material with remarkable electronic, mechanical and thermal properties. Owing to its 2D structure, all the delocalized π-conjugated electrons are effectively available on the surface which makes its electronic structure very sensitive to the local chemical environment. Thus it is an ideal material for sensing applications with large surface to volume ratio and low cost [8]. Choi et al reported the preparation of free-standing, flexible, conductive and reduced graphene oxide/Nafion (RGON) hybrid films for electrochemical biosensing of organophosphate (OP) detection. The self-assembly of sodium dodecyl benzene sulphonate (SDBS) functionalized graphene sheets and horseradish peroxidase (HRP) was reported by Zeng et al to display the high electrocatalytic activity towards H_2O_2 with high sensitivity [9-10]. Several studies have been reported in the construction of electrochemical biosensors using graphene oxide modified electrodes [11-18]. Qian et al reported that polypyrrole-reduced graphite oxide core-shell microspheres for electrochemical detection of dopamine in nanomolar concentrations and Bagherzadeh et al reported that electrochemical detection of dopamine based on pre-concentration by graphene nanosheets prepared by glucose reduction [19-20]. Most of these techniques are based on prior chemical reduction of graphene oxide and has been used for electrochemical sensing of DA and other molecules. Wang et al used direct electrochemical reduction of single-layer graphene oxide and its subsequent functionalization with Glucose Oxidase. Ping *et al* studied the direct electrochemical reduction of graphene oxide on ionic liquid doped screen-printed electrode and its electrochemical biosensing application [21-24]. More recently, Casero et al reported that GO could be electrochemically reduced completely

to graphene in aqueous solution without any dangerous chemicals for the development of biosensing platforms with improved analytical performance [25]. Zhang et al used electrochemical reduction method for completely reducing the graphene oxide by cycling the electrode in 0.5 M Na_2SO_4 aqueous solution for 20 cycles for non-enzymatic glucose sensing [26]. Recently, Liu et al reported electrochemically reduced graphene oxide functionalized with poly (o-phenylenediamine) for electrochemical sensing of dopamine with detection limit of 7.5×10^{-6} M [27]. But these works make use of the complete electrochemical reduction of graphene oxide by large number of potentiodynamic cycling or several hours for potentiostatic reduction procedures which are laborious for sensing application. Kong et al studied the influence of different oxygenated groups on graphene oxide's catalytic performance. Their basal plane is covalently surrounded by epoxy and hydroxyl groups while the edges are decorated with carboxyl groups. Even after reduction for achieving graphene, these functional groups are inevitable and cannot be removed completely [28].

The goal of this work is to synthesize electrochemically partially reduced graphene oxide by controlling the number of potentiodynamic cycling and potential window in aqueous phosphate buffered medium at pH 3.0. This resulted in better selectivity and sensitivity for individual and simultaneous determination of AA, DA and UA without any further modification. The developed electrode was successfully applied to human serum samples for recovery studies of physiologically related species AA, DA and UA.

2. Experimental section

2.1 Chemicals and reagents

Graphite powder, dopamine (DA), ascorbic acid (AA), uric acid (UA) and potassium ferricyanide were purchased from Aldrich, Milwaukee, WI, USA. All other chemicals such as concentrated H_2SO_4, fuming HNO_3, HCl, $KMnO_4$, 30% H_2O_2 were of analytical reagent grade (E Merck, Mumbai, India) and were used as received without further purification. All

stock solutions and working solutions were prepared using double distilled water. 0.1 M of phosphate buffer solution (adjusted to pH 3.0 with HCl) was used as supporting electrolyte in all electrochemical experiments. Stock solution of 0.1 M of ascorbic acid, dopamine and uric acid were prepared for each series of experiments.

2.2 Instrumentation

Electrochemical experiments were carried out in a conventional three-electrode cell at room temperature using a potentiostat/galvanostat μ-Autolab system (Ecochemie, Netherlands). The system was run on a PC using GPES 4.9 software. Working electrode was GC disc of surface area 0.071 cm^2. Reference electrode and counter electrode used were Ag/AgCl (in saturated KCl solution) and platinum foil, respectively. The size and morphology was studied by scanning electron microscope (SEM), JEOL, Model JSM 5600 LV, Tokyo, Japan and high-resolution transmission electron microscopy (HRTEM) on a FEI, TECNAI 30G2 S-TWIN microscope with an accelerating voltage of 300 kV.

2.3 Electrochemical measurements

Appropriate amounts of fresh solutions of AA, DA and UA were added to an electrochemical cell containing 0.1 M phosphate buffer medium at pH 3 and then three electrode systems were installed on it. Differential pulse voltammograms (DPV) were drawn by scanning the potential from -0.20 to +0.80 V with voltage step of 5 mV, modulation time of 0.25 s and modulation amplitude of 100 mV, respectively. The individual and simultaneous determination of AA, DA and UA were achieved by measuring the oxidation peak currents with respect to the concentration of respective analytes.

3. Results and discussion

3.1 Graphite oxide preparation

Graphite oxide was synthesized by modified Hummer's method using graphite powder as the precursor as previously reported [29]. Typically, 5.0 g of graphite powder (<45

mm, Sigma-Aldrich) was added into 180 mL of concentrated H_2SO_4 and stirred for 1 h in a fume hood. Then 60 mL of fuming HNO_3 was slowly added to the mixture under ice-cooling and stirring. After cooling down, 25 g of $KMnO_4$ was slowly added under ice-cooling and stirring. The mixed slurry was stirred at room temperature in a fume hood for 120 h. After that, 600 mL of deionized water was slowly added into the reacted slurry and stirred for 2 h; then 30 mL of 30% H_2O_2 was added, and the slurry immediately turned into a bright yellow solution with bubbling. Supernatant solution was decanted and resultant yellow slurry was centrifuged and then washed in 1000 mL of deionized water with 5 mL of HCl (37%) and 3 mL of 30 % H_2O_2 added. After stirring for 2 h, the solution was centrifuged and then washed again. This process was repeated three times. After that, the yellow slurry was further washed with 500 mL of deionized water until the pH of the washing solution increased to neutral (~ 6.5) (it requires about 500 mL×12 washes). The remaining dark-yellow solid was dried under vacuum at 40 ^{o}C for 48 h and ground to fine powder. The drying process for graphite oxide must be carried out at low temperatures because it slowly decomposes (deoxygenates) above 60 to 80 ^{o}C.

3.2 Construction of electrochemically reduced RGO-GCE

Chemically prepared graphite oxide was first exfoliated in double distilled water. A total of 20 mg of preformed graphite oxide was mixed with 20 mL of deionized water and ultrasonicated for 1 h. GO is hydrophilic and dispersible in aqueous media owing to the presence of oxygen containing functional groups. The resultant homogeneous yellow-brown GO nanosheet solution in water is stable for three to four months. GCE was polished successively using 0.30 μm and 0.05 μm Al_2O_3 powder and rinsed thoroughly with ethanol and water each for 5 min, and dried in air. Approximately 7 μL of the above suspension (1 mg mL^{-1}) was then pippetted onto the polished GCE surface and dried at room temperature for 30 minutes. In order to electrochemically reduce the GO nanosheet coated on GCE, the

GO modified electrode was cycled twice between the potential range starting from 0.00 V and with first vertex potential of -0.90 V and second vertex potential of +0.80 V with a scan rate of 50 mVs^{-1} in phosphate buffer solution adjusted to pH 3.0 as shown in **Fig. 1**.

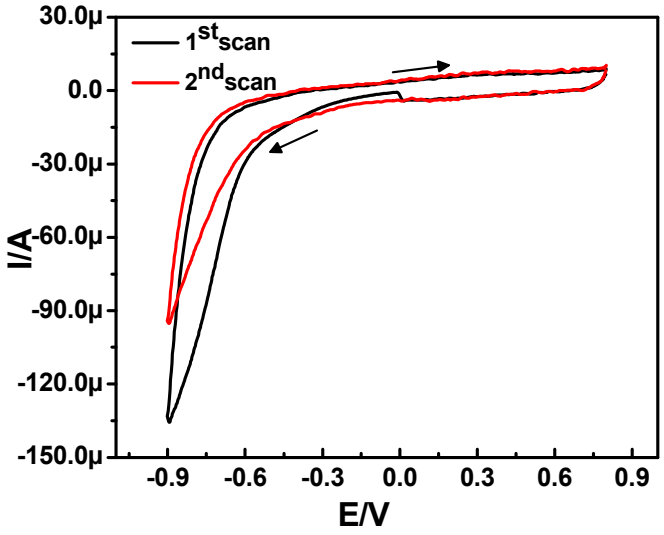

Fig. 1 Cyclic voltammograms of the electrochemical reduction of GO drop casted on GCE in 0.1 M phosphate buffer (pH 3.0) at the scan rate of 50 mVs^{-1}.

3.3 Electrochemical behaviour of AA, DA and UA at different modified electrodes.

The electrochemical behaviour of RGO-GCE was first tested with cyclic voltammetry for its response to AA, DA and UA and identified the role of electrochemical reduction of chemically synthesised GO. Fig. 2 (a & b) shows the cyclic voltammograms at a scan rate of 50 mVs^{-1} and DPV curves for AA, DA and UA in a potential range of -0.20 to 0.80 V with 0.1 M of phosphate buffer solution at pH 3.0 as supporting electrolyte. At the modified electrode the oxidation peaks of AA, DA and UA are sensitive and well resolved while dopamine peak showed enhanced analytical signal owing to the enrichment via adsorption offered by the RGO-GCE. At pH 3.0, the oxidized species of AA & UA do not interfere during the determination of DA.

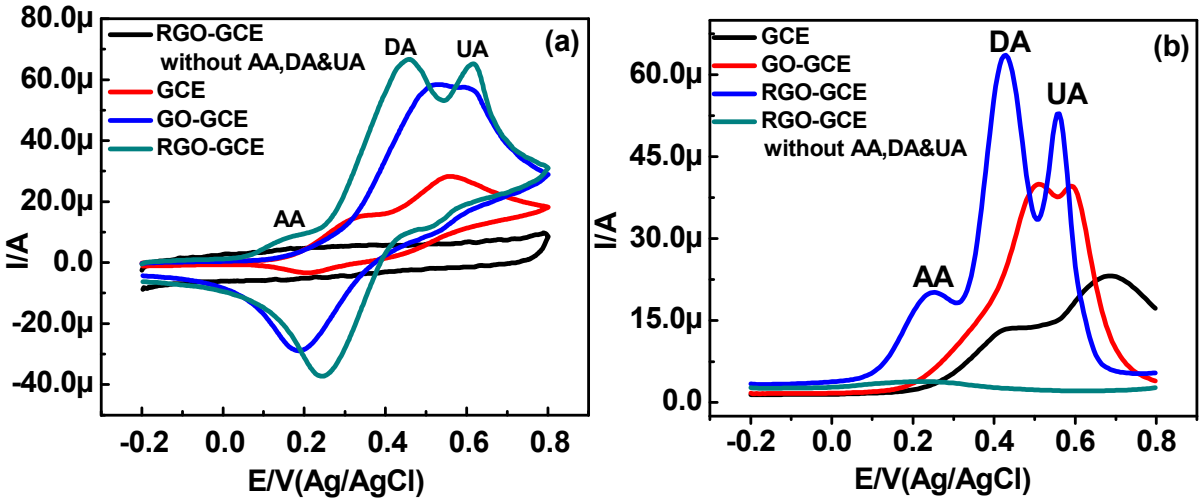

Fig. 2 (a) Cyclic voltammetric responses of AA, DA and UA (each 1×10^{-3} M, scan rate 50 mVs^{-1}) at GCE, GO-GCE and RGO-GCE modified electrodes (b) corresponding DPV curves (each1×10^{-3} M, DPV conditions: -0.20 to +0.80 V, 0.1M phosphate buffer pH 3.0).

3.4 Characterization of GO-GCE and RGO-GCE

3.4.1 Morphological characterization.

The surface morphology of the material was examined through a scanning electron microscope (SEM) and a transmission electron microscope (TEM). **Fig. 3 (A, B, C & D)** shows the TEM and SEM images of graphene oxide nano sheets (A & C) and electrochemically reduced graphene oxide nano sheet (B & D), respectively. As shown in the figures, the graphene oxide nanosheets were transparent and wrinkled in nature. This wrinkled nature of graphene oxide is highly beneficial in maintaining a high surface area of the electrode since the sheets cannot readily collapse back to a graphitic structure.

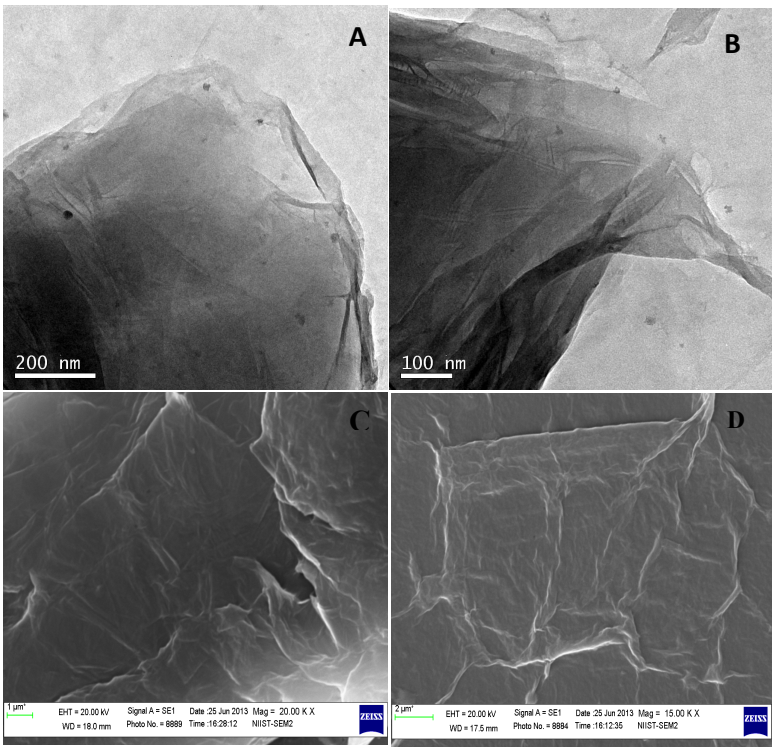

Fig. 3 TEM and SEM images of GO (A& C) and RGO (B & D) respectively (GO and RGO are formed as per procedures described in experimental section.

3.4.2 FT-IR

FT-IR spectra of graphene oxide nano sheet and partially reduced graphene oxide nano sheet are shown in **Fig. 4**. IR spectrum of graphene oxide (curve A) indicates the presence of oxygen functionalities such as epoxide, hydroxyl and carbonyl functional groups on the layers. A strong broad stretching vibration due to the hydroxyl groups (-C-OH) is observed at 3300 cm^{-1} and a weak band due to -C=O stretching vibrations of -COOH group is observed at 1720 cm^{-1}. The strong band at 1390 cm^{-1} is assigned to the O−H deformations of the C−OH groups and the band at 1040 cm^{-1} is due to C-O stretching vibrations of alkoxy group. Peak at ~1620 cm^{-1} corresponds to O-H stretching vibrations. After the electrochemical reduction of the exfoliated GO, the C=O vibration band disappears, the O-H stretching vibrations bands remain (curve B) [28].

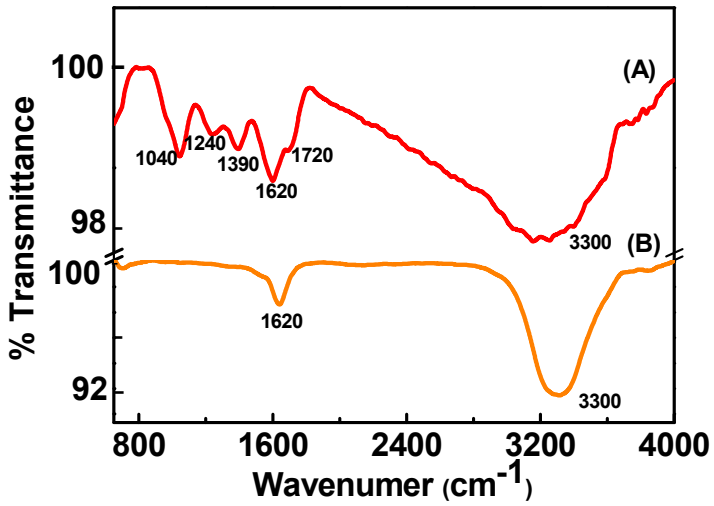

Fig. 4 FT-IR spectra of GO (A) and RGO (B) materials.

3.4.3 Raman spectra

In order to get the idea about ordered and disordered structures of carbon in the graphite, GO and RGO, Raman spectra were investigated (**Fig. 5**). Graphite displays a strong G band at 1578 cm^{-1}, which is assigned to the E_{2g} phonon of sp^2 carbon atoms. While a prominent D band at 1350 cm^{-1} appeared in GO, which corresponds to the breathing mode of k-point phonons of A_{1g} symmetry. The emergence of D band indicates the existence of defects in GO caused by oxidation. When GO was electrochemically reduced to RGO, the D/G intensity ratio increases obviously, suggesting a decrease in the average size of sp^2domains [30, 31].

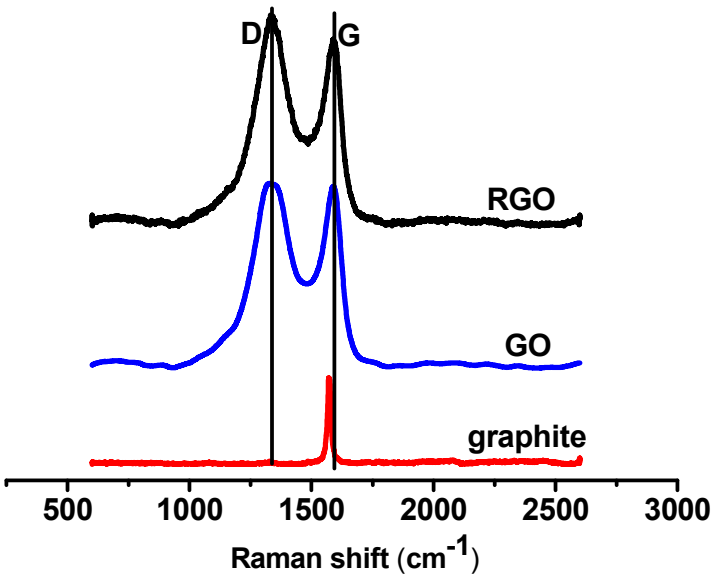

Fig. 5 Raman spectra of graphite, GO and RGO

3.5 Electrochemical characterization

3.5.1 Electrochemical behaviour of GO and RGO modified GCE in $K_3[Fe(CN)_6]$

To investigate the electrochemical behaviour of bare GCE, GO-GCE and RGO-GCE, the cyclic voltammetric experiments were carried out by using $K_3[Fe(CN)_6]$ as the electrochemical probe. The cyclic voltammograms of bare GCE, GO and RGO-GCE electrodes in 5×10^{-3} M $K_3[Fe(CN)_6]$ with 0.1 M KCl as the supporting electrolyte are shown in **Fig. S1**. At the bare GC electrode, the peak potential difference of (ΔEp) 101mV indicates a quasi-reversible redox reaction. At the GO-GCE a decreased current response was observed with ΔEp of 149 mV, because of the presence of oxygen functionalities on the graphene oxide which will repel the negatively charged ferricyanide probe. During electrochemical reduction, the oxygen functionalities such as epoxy, carboxylic acid and aldehyde groups in graphene oxide nanosheet were reduced partially. This results in more conductive partially reduced graphene oxide nanosheet with some hydroxyl groups and having conductivity better

than GO nanosheet. After reduction ΔEp became 131 mV with increase in current indicating modification of GO and its partial reduction to RGO film on GCE.

3.5.2 Kinetic studies

3.5.2.1 Effect of scan rate

The effect of scan rate on the CV responses of AA, DA and UA at RGO-GCE was studied. **Fig. S2 (A, B & C)** shows the oxidation peak currents of AA, DA and UA which increases with increasing scan rate because in short scale experiments, there is a time constraint for catalytic reaction to take place completely, while their oxidation peak potentials gradually shift to positive values suggesting a kinetic limitation in the reaction between the redox sites of the modified electrode and small physiologically related molecules. Plots of anodic peak currents (Ip) as a function of the square root of scan rate variation ($\upsilon^{1/2}$) in the range of 10-100 mVs^{-1} shows better linearity relationship compared to Ip vs υ, which indicates that electrode reactions of these three molecules are diffusion-controlled processes. On the basis of the slopes of the linear dependence of the anodic peak currents on the square root of the potential sweep rates, by the Randles-Sevcik equation

$$Ip = (2.99 \times 10^5)\, \alpha^{0.5}\, n^{1.5}\, ACD^{0.5}\, \upsilon^{0.5}$$

where Ip is the peak current, A is the electrode surface area, D is the diffusion co-efficient and C is the bulk concentration. Using above equation the diffusion coefficients of AA, DA and UA for RGO-GCE modified electrode was calculated to be 4.0×10^{-6}, 3.8×10^{-8} and 1.9×10^{-8} $cm^2\, s^{-1}$, respectively.

In order to obtain information about the rate determining step, the Tafel plot was drawn using the following equation, for a diffusion controlled process,

$$E_p = (2.303RT/2n\alpha F) \log \upsilon + \text{constant}$$

Based on the above equation, from the Tafel plot the slopes of E_p vs. log υ for the RGO-GCE modified electrode for AA, DA and UA was found to be 0.030, 0.040 and 0.039, respectively.

These slopes give the values of electron transfer co-efficient α as 0.46, 0.36 and 0.37 for a two electron transfer process, which is the rate determining step.

The electron transfer co-efficient for the oxidation of AA, DA and UA at pH 3.0 at modified electrodes can also be calculated by using Laviron's equation for a quasi-reversible system,

$$n\alpha = 0.048/Ep\text{-}E_{p/2}$$

where $E_{p/2}$ is the potential corresponding to $I_{p/2}$.The values of α were found to be 0.54, 0.34 and 0.46 assuming n=2 for the oxidation of AA, DA and UA at the surface of the RGO-GCE, which matches with those obtained from Tafel plot.

3.5.2.2 Chronoamperometric experiments

Single step potential chronoamperometry was also employed to investigate the electrochemical process at the chemically modified electrode. **Fig. S3 (A, B and C)** shows the current-time curves of RGO-GCE for AA, DA and UA, respectively by setting the working electrode potential at +0.60 V in buffered aqueous solutions of pH 3.0. The chronoamperometry of the modified electrode in the presence of physiologically related species represents a typical I-t curve, which indicates diffusion controlled process. The rate constants for the AA, DA and UA oxidations can also be evaluated by chronoamperometry according to the equation

$$I_C/I_L = \pi^{1/2}(kCt)^{1/2}$$

From the plot of I_C/I_L vs $t^{1/2}$ the rate constants for AA, DA and UA were found to be 3.14×10^6, 6.8×10^5 and 6.6×10^4 mol cm^{-3} s^{-1}, respectively for the RGO-GC electrode.

3.6 Optimization of experimental and analytical parameters.

The RGO modified electrode's response towards adsorbed DA is dependent on the amount of GO drop casted onto the glassy carbon electrode, number of reduction cycles and the potential range. Therefore, different amount of GO (3, 5, 7 and 10 µL of the homogenized 1 mg mL^{-1} GO suspension) were cast on the glassy carbon electrode and optimized to 7µL (m

(GO) = 7 mg, note that 'm' refers to the mass of GO) of GO suspension. Another important parameter which depends upon the sensitivity of the modified electrode towards dopamine sensing is the electrochemical reduction of GO. To obtain the partial reduction of the oxygen functionalities on the GO nanosheets, the cathodic potential scan limit was varied from -0.50 to -1.20 V and optimized to -0.80V. Anodic potential scan limit does not play a crucial role in the sensing of DA and was optimized to +0.90 V after varying from +0.50 V to +1.20 V. Number of potentiodynamic cycling under optimized scan limits was varied from 1, 2, 4, 15 and 25 cycles and optimized for 2, with a scan rate of 50 mVs^{-1}.

The effect of solution pH on the CV responses of 1×10^{-3} M AA, DA and UA at RGO-GCE were studied in phosphate buffer by varying the pH from 3.0 to 9.0 in steps of 2.0. From the **Fig. S4 (a)** it can be observed that for DA, both the anodic and cathodic peak potentials shifted negatively and cathodic peak current decreases (formation of polydopa) with increase of pH, indicating that the redox reaction of DA include protons transferred at the RGO modified electrode. The plot of Ep_a versus pH displays linearity in the pH range of 3.0-9.0 with a slope of -60 mV pH^{-1} (**Fig. S4 (b))** and the slope value is very close to the theoretical value of -59 mV pH^{-1}, suggesting that the electrocatalytic oxidation of DA at the RGO-GCE involves an equal number of electrons and protons. The influence of pH on the anodic peak current of AA, DA and UA were studied and observed that maximal anodic current responses were obtained at pH 3.0 for AA and UA, but for DA it was pH 7.0. For enabling the simultaneous determination of the analytes the pH of the medium were fixed at 3.0 for further studies, even though pH 7.0 gives maximum anodic peak current for DA. Accordingly, 0.1 M phosphate buffer of pH 3.0 was selected for all subsequent experiments in this study.

The dependence of the oxidation peak current of dopamine on the enrichment time at the RGO-GCE was studied. The RGO-GCE was immersed in 0.1 M phosphate buffer at pH = 3.0 containing 1×10^{-3} M of DA and the solution was stirred for different time periods ranging

from 60 to 300 s in steps of 60 s. The DPV response signal for DA enrichment was increased with increased enrichment time and then reached equilibrium after about 3 minutes. Since RGO-GCE contain hydroxyl groups, the dopamine get preconcentrated by electrostatic interaction in short time period of three minutes compared to 20 min recently reported by Bagherzadeh et al [20] on graphene modified electrode.

The dopamine peak current of differential pulse voltammogram is also dependent on the instrumental parameters. The instrumental parameters are interrelated and can be optimized by monitoring the peak current as a function of parameter values, while other parameters are fixed. The optimized instrumental conditions are modulation amplitude (100 mV), voltage step (5 mV), and modulation time of 0.25 s.The investigated and optimized experimental conditions are summarized in **Table 1.**

Table 1: Investigated and optimal conditions of electrochemical partial reduction of GO and analytical parameters for the determination of AA, DA and UA using RGO-GCE.

Parameters	Investigated Range	Optimal conditions
(A) Electrochemical partial reduction		
Amount of GO (mg mL^{-1})	3 to 10	7
Number of cycles	0 to 25	2
Cathodic potential scan limit(V)	- 0.50 to -1.20	-0.80
Anodic potential scan limit (V)	+0.50 to +1.20	+0.90
(B) Differential pulse voltammetric sensing of AA, DA and UA in 0.1M Phosphate buffer		
pH	3.0-9.0	3.0
Enrichment time (s)	60-300	180
Modulation amplitude (mV)	10 to 200	100
Voltage step (mV)	1 to 10	5
Modulation time (s)	0.1 to 0.5	0.25
Start potential (V)	-0.50 to 0.10	-0.20
End potential (V)	0.70 to 1.10	0.80

3.7 Individual and simultaneous determination of AA, DA and UA with RGO-GCE

Individual determination of AA, DA and UA at RGO-GCE were carried out at optimal conditions of DA, in the potential range of -0.20 to 0.60 V in phosphate buffer (pH 3.0). During the measurements, only the concentrations of the target molecule were varied, while concentrations of the other two analytes were kept constant. As shown in **Fig. 6 (a, b & c)** the electrochemical responses of AA, DA and UA increases linearly with the increase in concentrations of the respective target analyte. When compared with GCE, the presence of functional groups on RGO-GCE reduces the anodic over potentials and exhibits well-defined oxidative peaks for AA, DA and UA (0.16, 0.45 and 0.62 V). Hence, the peak separations between DA-AA (0.30 V), UA-DA (0.17V) and AA-UA (0.46V) is sufficient enough to give three separate peaks. A linear calibration range of 4×10^{-5} to 1×10^{-3} M of AA in presence of 1×10^{-5} M DA and 1×10^{-4} M UA was obtained with a correlation coefficient of 0.982 and detection limit of 4.2×10^{-6} M (based on 3 times the standard deviation of the blank). DA shows a linear calibration range from 1×10^{-7} to 1.7×10^{-4} M in presence of 1×10^{-3} M each of AA and UA with correlation coefficient of 0.995 (lower levels) and 0.998 (higher levels) with detection limit of 8×10^{-9} M. In the case of UA, it has three linear calibration range, one lower (8×10^{-7} to 8×10^{-6} M), middle (1×10^{-5} to 1×10^{-4} M) and upper (2×10^{-4} to 8×10^{-4} M) with correlation coefficients of 0.996, 0.996 and 0.999, respectively in presence of 1×10^{-5} M of DA and 1×10^{-4} M of AA and has a detection limit of 6×10^{-7} M. It is also found that, the addition of target molecules into the electrochemical cell does not have significant influence on the peak currents and peak potentials of the other two biomolecules. The modified electrode was stable for weeks and has a precision of 1.42, 1.92 and 2.20% for AA, DA and UA with limit of quantification (LOQ) of 1.4×10^{-5}, 2.7×10^{-8}, 2.0×10^{-6} M, respectively.

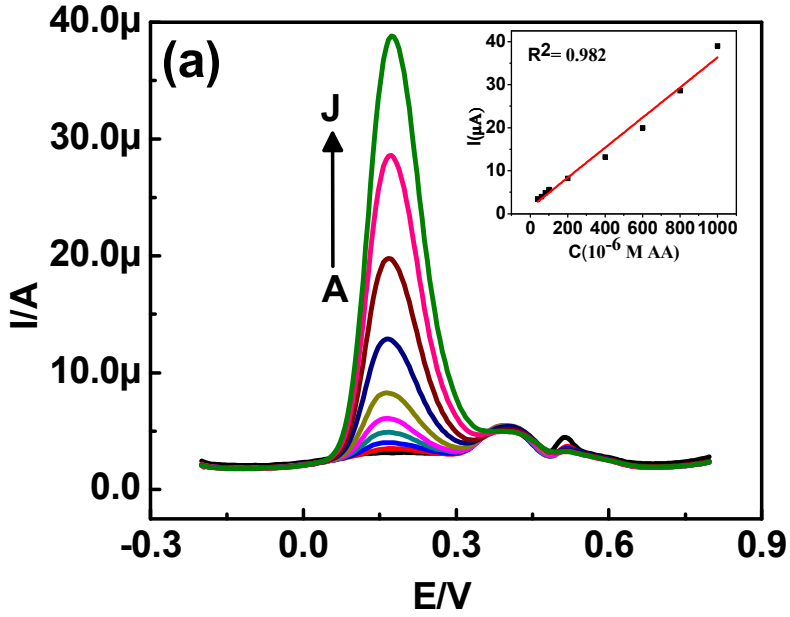

Fig. 6 (a) DPV profiles of AA in presence of 1×10^{-4} M of UA and 1×10^{-5} M of DA at different concentrations: 0, 4×10^{-5}, 6×10^{-5}, 8×10^{-5}, 1×10^{-4}, 2×10^{-4}, 4×10^{-4}, 6×10^{-4}, 8×10^{-4} and 1×10^{-3} M (A to J) Inset: corresponding calibration plot.

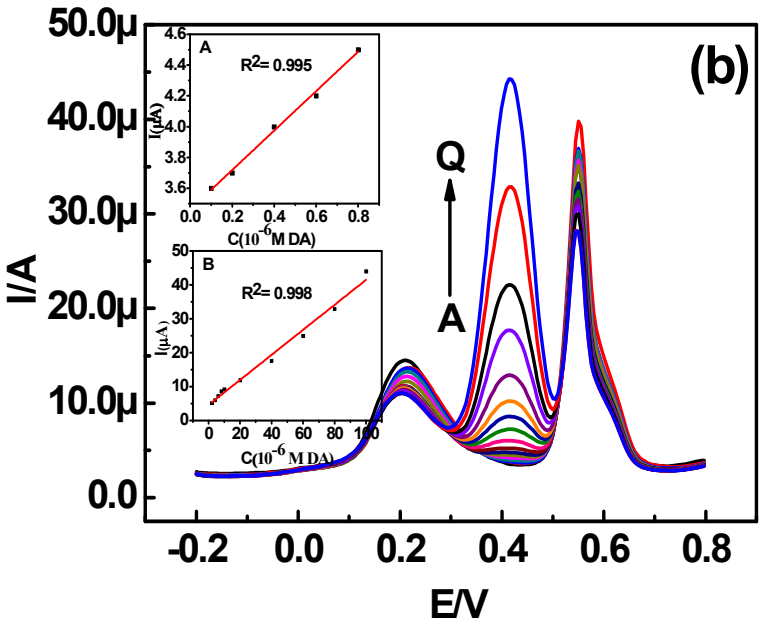

Fig. 6 (b) DPV profiles of DA in presence of 1×10^{-3} M each of AA and UA at different concentrations: 0, 1×10^{-7}, 2×10^{-7}, 1×10^{-7}, 6×10^{-7}, 8×10^{-7}, 1×10^{-6}, 2×10^{-6}, 4×10^{-6}, 6×10^{-6}, 8×10^{-6}, 1×10^{-5}, 2×10^{-5}, 4×10^{-5}, 6×10^{-5}, 8×10^{-5} and 1×10^{-4} M (A to Q) Inset: corresponding calibration plots for lower & higher concentrations.

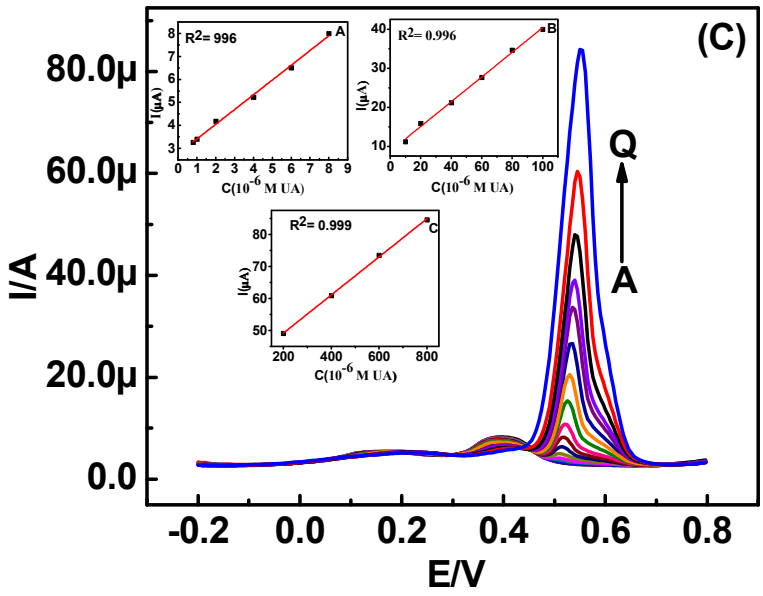

Fig. 6 (c) DPV profiles of UA in presence of 1×10^{-5} M of DA and 1×10^{-4} M of AA at different concentrations: 0, 8×10^{-7}, 1×10^{-6}, 2×10^{-6}, 4×10^{-6}, 6×10^{-6}, 8×10^{-6}, 1×10^{-5}, 2×10^{-5}, 4×10^{-5}, 6×10^{-5}, 8×10^{-5}, 1×10^{-4}, 2×10^{-4}, 4×10^{-4}, 6×10^{-4} and 8×10^{-4}M (A to Q) Inset: corresponding calibration plots for lower (A), middle (B) & higher concentrations (C).

Fig. 7 (a, b, c & d) shows the DPV profiles and corresponding calibration plots for the simultaneous determination of AA, DA and UA, respectively using RGO-GCE. It has a linear calibration range of 1×10^{-5} to 1.2×10^{-3} M for AA and UA, and for DA it was 1×10^{-6} to 1.2×10^{-4} M. This result demonstrates that individual or simultaneous determination of AA, DA and UA can be achieved with high sensitivity and equally good resolution on RGO-GCE.

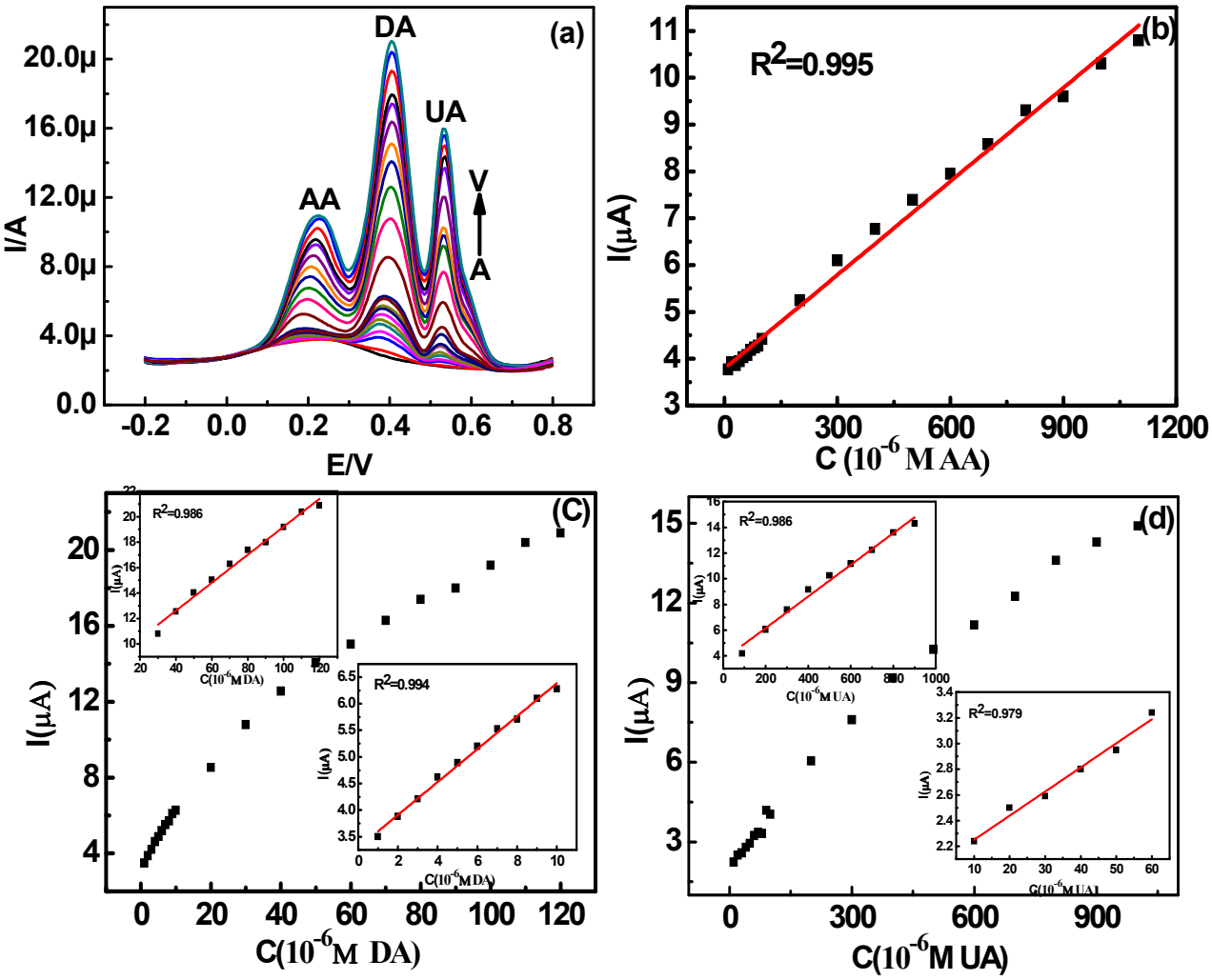

Fig. 7 (a) DPV profiles at RGO-GCE in 0.1 M phosphate buffer (pH 3.0) containing different concentrations of AA, DA and UA (A-V). Concentrations are ranging from 1×10^{-5} to 1.2×10^{-3} M for AA and UA, 1×10^{-6} to 1.2×10^{-4} M for DA, respectively**. (b)-(d)** Plots of the oxidation peak currents as a function of AA, DA and UA concentrations, respectively**.**

3.8 Influence of repetitive voltammetric cycling

Many of the studies in voltammetric detection of DA have focused on the use of carbon-based electrode materials because of its desirable range of properties. However, most carbon electrodes are highly susceptible to fouling. It is widely appreciated that DA electro-oxidation can leads to rapid fouling and results in contamination of working electrode

surfaces. Unwin et al studied the electro-oxidation of dopamine on the unmodified surface of five different classes of carbon electrodes and observed that extent and rate of electrode fouling are dependent on the electrode material [32]. We have examined the extent to which the fouling effect causes the sensitivities of AA, DA and UA with RGO-GCE and bare GCE by recording consecutive CVs (typically 10 at a scan rate of $0.1Vs^{-1}$) at pH 3.0 & 7.0**. Fig. S5** shows typical CVs for repetitive cycling in 1×10^{-3} M DA (0.1M phosphate buffer, pH 3.0 & 7.0) using RGO modified and bare GC electrode. The repetitive CVs of RGO-GCE and bare GCE show that fouling effect was observed at pH 7.0 and was absent in pH 3.0 irrespective of the electrode. It may be due to the fact that at neutral or basic pH the electro-oxidation of dopamine causes the formation of polydopa on the surface of the electrode and reduces the sensitivity of the modified electrode with increase in scan number. Furthermore we have examined the effect of electro-oxidation AA and UA (individually and together) towards the sensitivity of dopamine determination by repetitive CVs and DPVs at pH 3.0 phosphate buffered medium under optimized conditions. **Fig. S6 (A, B & C)** shows the repetitive CVs for the electro-oxidation of dopamine in presence of 1×10^{-3} M each of AA and UA and both. To obtain the percentage decrease of current signals corresponding DPV profiles were also drawn under optimized conditions (**Fig. S6 D).** It can be inferred that as the number of scan increases, the sensitivity of the dopamine is only slightly affected (~ 8%). But with increase in scan number the sensitivity of AA and UA are severely affected due to the electro-oxidation of dopamine.

3.9 Real sample analysis

To establish the applicability of the developed sensor, the electrode was tested for the simultaneous determination of AA, DA and UA added to a serum samples suitably diluted in the experimental buffer medium and the recovery measurements were carried out. Serum samples were obtained from Amrita Institute of Medical Science and Research centre,

Cochin, Kerala, India. Briefly, 5 mL of human blood was centrifuged (1000 rpm for 20 minutes) to remove plasma. Appropriate aliquot (200 µL) of clear serum samples was used for the analysis of UA and recovery studies of small biomolecules such as AA and DA. The diluted serum samples have $3.4\pm1\times10^{-5}$ M of UA, and concentrations of AA and DA are below the detection limits of the developed procedure. Recovery studies were performed by spiking known amounts of standard solutions of AA, DA and UA to the diluted (100 times) serum samples followed by the analysis using the modified electrode under optimized analytical conditions. The results obtained are compiled in **Table 2**. The recoveries for AA, DA and UA in three different concentration levels lies in the range of 92-110 % indicating that there is no significant interference from the serum sample matrix. Thus, the developed sensor can find routine application to serum samples containing micromolar levels of AA, DA and UA simultaneously.

Table 2. Analysis of serum samples [200µL of serum sample is spiked with three different concentrations of AA, DA and UA (I, II & III)]. Optimized conditions for DPV: Enrichment time=180 s; 0.1 M phosphate buffer (pH 3.0); scan range from -0.20 to +0.80V. (BDL: Below detection limit)

Serum sample	Found (10^{-6}M)			Spiked (10^{-6}M)			Recovery (10^{-6}M)			% Recovery		
	AA	DA	UA	AA	DA	UA	AA	DA	UA	AA	DA	UA
I	BDL	BDL	34.0	100	10	10	98±1.4	9.9±0.7	43.8±0.3	98	99	98
II	BDL	BDL	35.0	250	25	25	251±0.2	24.8±0.2	59.5±0.1	100.2	99.2	102
III	BDL	BDL	34.0	500	50	50	492±0.2	50.4±0.2	84.6±0.7	98.4	100.8	101.2

3.10 Comparison with reported analytical procedures

The characteristic sensing features such as simplicity, limit of detection, linear calibration range etc of the developed sensor were compared with recently reported electrochemical sensors for simultaneous/Individual determination of AA, DA and UA are

shown in **Table S1**. The developed sensor, RGO-GCE shows comparatively better limit of detection (LOD) and has wider range of linear response for DA when compared with existing electrochemical sensors. The excellent electrocatalytic activity of the electrochemically partially reduced graphene oxide nanosheet promises a simultaneous determination of AA, DA and UA using the RGO-GCE.

4. Conclusions

In summary, a simple and partially reduced graphene oxide nanosheet modified electrode was designed based on the electrochemical reduction of exfoliated graphite oxide obtained from chemically formed graphite oxide and was used for individual and simultaneous detection and quantification of AA, DA and UA (LOD = 4.2×10^{-6}, 8×10^{-9}, 6×10^{-7} M and LOQ = 1.4×10^{-5}, 2.7×10^{-8}, 2.0×10^{-6} M, respectively). In addition, the modified electrode shows better enrichment, good resolution and precision (1.42, 1.92 and 2.20% for AA, DA and UA, respectively) paving the way for their simultaneous determination. Finally, this work provides the promising strategy for individual & simultaneous determination of AA, DA & UA in the presence of other co-existing species in biological fluids.

Acknowledgements

The authors thank Mrs. Lucy Paul for SEM analysis and Mr. Kiran for TEM analysis. Mr. P. K. Aneesh and Ms. Sindhu R. Nambiar are thankful to UGC and CSIR, New Delhi, India for the award of Senior Research Fellowships. Dr T. PrasadaRao is thankful to CSIR, New Delhi, India for providing funds through the MULTIFUN project (CSC0101).

REFERENCES

[1] O. Arrigoni and M. C. D. Tullio, *Biochim. Biophys. Acta*, 2002, **1569**, 1.

[2] J. H. Kim, J. M. Auerbach, J. A. R. Gomez, I. Velasco, D. Gavin, N. Lumelsky, S. H. Lee, J. Nguyen, R. S. Pernaute, K. Bankiewicz and R. McKay, *Nature*, 2002, **418**, 50.

[3] V. S. E. Dutt and H. A. Mottola, *Anal. Chem*., 1974, **46**, 1777.

[4] S. Hou, M. L. Kasner, S. Su, K. Patel and R. Cuellari**,** *J. Phys. Chem. C*, 2010, **114**, 14915.

[5] A. A. Ensafi, M. Taei and T. Khayamian, *J. Electroanal. Chem.*, 2009, **633**, 212.

[6] Y. Wu, L. Cui, Y. Liu, G. Lv, T. Pu, D. Liu and X. He, *Analyst*, 2013, **138**, 1204.

[7] K. S. Novoselov, A. K. Geim, S. V. Morozov, D. Jiang, Y. Zhang, S. V. Dubonos, I. V. Grigorieva and A. A. Firsov, *Science*, 2004, **306**, 666.

[8] S. Roy, N. Soin, R. Bajpai, D. S. Misra, J. A. McLaughlinb and S. S. Roy, *J. Mater. Chem*., 2011, **21**, 14725.

[9] B. G. Choi, H. S. Park, T. J. Park, M. H. Yang, J. S. Kim, S. Y. Jang, N. S. Heo, S. Y. Lee, J. Kong and W. H. Hong, *ACS Nano*, 2010, **4**, 2910.

[10] Q. Zeng, J. Cheng, L. Tang, X. Liu, Y. Liu, J. Li and J. Jiang, *Adv. Funct. Mater*., 2010, **20**, 3366.

[11] M. Zhou, Y. Zhai and S. Dong, *Anal. Chem*., 2009, **81**, 5603.

[12] S. Alwarappan, A. Erdem, C. Liu and C. Zhong Li, *J. Phys. Chem.* C, 2009, **113**, 8853.

[13] H. Wu, J. Wang, X. Kang, C. Wang, D. Wang, J. Liu, I. Aksay and Y. Lin, *Talanta*, 2009, **80**, 403.

[14] F. Bonaccorso, Z. Sun, T. Hasan and A. C. Ferrari, *Nature Photonics*, 2010, **4**, 611.

[15] M. I. Hoffert, K. Caldeira, G. Benford, D. R. Criswell, C. Green, H. Herzog, A. K. Jain, H. S. Kheshgi, K. S. Lackner, J. S. Lewis, H. D. Lightfoot, W. Manheimer, J. C. Mankins, M.

E. Mauel, L. J. Perkins, M. E. Schlesinger, T. Volk and T. M. L. Wigley, *Science*, 2002, **298**, 981.

[16] M. Pumera, *The Chemical Record*, 2009**, 9**, 211.

[17] Y. Y. Shao, J. Wang, H. Wu, J. Liu, I. A. Aksay and Y. H. Lin, *Electroanalysis*, 2010, **22**, 1027.

[18] A. Bonanni, A. H. Loo and M. Pumera, *Trends in Analytical Chemistry*, 2012, **37,** 12.

[19] T. Qian, S. Wu and J. Shenab, *Chem. Comm*., 2013, **49**, 4610.

[20] M. Bagherzadeh and M. Heydari, *Analyst*, 2013, **138**, 6044.

[21] P. Si, H. L. Chen, P. Kannan and D. H. Kim, *Analyst*, 2011, **136**, 5134.

[22] Z. J. Wang, X. Z. Zhou, J. Zhang, F. Boey and H. Zhang, *J. Phys. Chem. C*, 2009, **113**, 14071.

[23] X. Y. Peng, X. X. Liu, D. Diamond and K. T. Lau, *Carbon*, 2011, **49**, 3488.

[24] J. F. Ping, Y. X. Wang, K. Fan, J. Wu and Y. B. Ying, *Biosens. Bioelectron*., 2011, **28**, 204.

[25] E. Casero, C. Alonso, L. Vazquez, M. D. Petit-Dominguez, A. M. Parra-Alfambra, M. de la Fuente, P. Merino, S. Alvarez-Garcia, A. de Andres, F. Pariente and E. Lorenzo, *Electroanalysis*, 2013, **25**, 154.

[26] Y. Zhang, X. Xiao, Y. Sun, Y. Shi, H. Dai, P. Ni, J. Hu, Z. Li, Y. Song and Li Wang, *Electroanalysis*, 2013, **25**, 959.

[27] X. Liu, H. Zhua and X. Yang, *RSC Adv*., 2014, **4**, 3706.

[28] X. Kong, Q. Chen and Z. Lun, *J. of Mater. Chem. - A*, 2014, **2**, 610.

[29] W.S. Hummers Jr and R. E. Offeman, *J. Am. Chem. Soc*., 1958, **80**, 1339.

[30] S. Stankovich, D. A. Dikin, R. D. Piner, K. A. Kohlhaas, A. Kleinhammes, Y. Y. Jia, Y. Wu, S. T. Nguyen and R. S. Ruoff, *Carbon*, 2007, **45**, 1558.

[31] Z. H. Ni, H. M. Wang, Y. Ma, J. Kasim, Y. H. Wu and Z. X. Shen, *ACS Nano*, 2008, **5** 1033.

[32] A. N. Patel, S.Tan, T. S. Miller, J. V. Macpherson, and P. R. Unwin, *Anal. Chem.*, 2013, **85**, 11755.

[33] W. Caia, T. Laia, H. Dub and J. Ye, *Sens. and Actuators B*, 2014, **193**, 492.

[34] J. Du, R. Yue, F. Ren, Z. Yao, F. Jiang, P. Yang and Y. Du, *Biosens. Bioelectron.*, 2014, **53**, 220.

[35] Y. J. Yang and W. Li, *Biosens. Bioelectron.*, 2014, **56**, 300.

[36] X. Liu, L. Zhang, S. Wei, S. Chen, X. Ou and Q. Lu, *Biosen. Bioelectron.*, 2014, **57**, 232.

[37] C. Wang, P. Xu, and K. Zhuo, *Electroanalysis*, 2014, **26**, 191.

[38] T. Xu, Q. Zhang, J. Zheng, Z. Lv, J. Wei, A. Wang and J. Feng, *Electrochim. Acta*, 2014, **115**, 109.

[39] D. Wu, Y. Li, Y. Zhang, P. Wang, Q. Wei and B. Du, *Electrochim. Acta*, 2014, **116**, 244.

[40] L. Yang, D. Liu, J. Huang and T. You, *Sens. and Actuators B*, 2014, **193**, 166.

[41] J. Zhang, Z. Zhu, J. Zhu, K. Li and S. Hua, *Int. J. Electrochem. Sci.*, 2014, **9**, 1264.

[42] Z. Zhang and J. Yin, *Electrochim. Acta*, 2014, **119**, 32.

[43] X. Wang, M. Wu, W. Tang, Y. Zhu, L. Wang, Q. Wang, P. He and Y. Fang, *J. Electroanal. Chem.*, 2013, **695**, 10.

[44] S. Yu, C. Luo, L. Wang, H. Peng and Z. Zhu, *Analyst*, 2013, **138**, 1149.

[45] Y. Wu, L. Cui, Y. Liu, G. Lv, T. Pu, D. Liu and X. He, *Analyst*, 2013, **138**, 1204.

[46] S. Zhou, H. Shi, X. Feng, K. Xue and W. Song, *Biosen. Bioelectron.*, 2013, **42**, 163.

[47] C. Xue, Q. Han, Y. Wang, J. Wu, T. Wen, R. Wang, J. Hong, X. Zhou and H. Jiang, *Biosens. Bioelectron.*, 2013, **49**,199.

[48] T. Qian, S. Wu and J. Shenab, *Chem. Comm.*, 2013, **49**, 4610.

[49] A. X. Oliveira, S. M. Silva, F. R. F. Leite, L. T. Kubota, F. S. Damos and R. C. S. Luz, *Electroanalysis*, 2013, **25**, 723.

[50] S. B. A. Barros, A. Rahim, A. A. Tanaka, L. T. Arenas, R. Landers and Y. Gushikem, *Electrochim. Acta*, 2013, **87**, 140.

[51] P. Gai, H. Zhang, Y. Zhang, W. Liu, G. Zhu, X. Zhang and J. Chen, *J. Mater. Chem. B*, 2013, **1**, 2742.

[52] L. Zhang, W. J. Yuan and B. Q. Hou, *J. Electroanal. Chem.*, 2013, **689**, 135.

[53] Y. Wang and C. Bi, *Journal of Molecular Liquids*, 2013, **177**, 26.

[54] Z. Temocin, *Sens. and Actuators B*, 2013, **176**, 796.

[55] X. Zheng, X. Zhou, X. Ji, R. Lin and W. Lin, *Sens. and Actuators B*, 2013, **178**, 359.

[56] W. Zhang, Y. Chai, R. Yuan, J. Han and S. Chen, *Sens. and Actuators B*, 2013, **183**, 157.

[57] X. Ma, M. Chao and Z. Wang, *Anal. Methods*, 2012, **4**, 1687.

[58] M. S. Hsu, Y. L. Chen, C. Y. Lee, and H. T. Chiu, *ACS Appl. Mater. Interfaces*, 2012, 4, 5570.

[59] Z. H. Sheng, X. Q. Zheng, J. Y. Xu, W. J. Bao, F. B. Wang, X. H. Xia, *Biosens. Bioelectron.,* 2012, **34**, 125.

[60] Q. Liu, X. Zhu, Z. Huo, X. He, Y. Liang and M. Xu, *Talanta*, 2012, **97**, 557.

[61] S. Shahrokhian, A. M. Shakib, M. Ghalkhani and R. Saberi, *Electroanalysis*, 2012, **24**, 425.

[62] D. Q. Huang, C. Chen, Y. M. Wu, H. Zhang, L. Q. Sheng, H. J. Xu and Z. D. Liu, *Int. J. Electrochem. Sci.*, 2012, **7**, 5510.

[63] D. Yuan, X. Yuan, S. Zhou, W. Zou and T. Zhou, *RSC Adv.*, 2012, **2**, 8157.

[64] M. Chao, X. Ma and X. Li, *Int. J. Electrochem. Sci.*, 2012, **7**, 2201.